International Journal of Mass Spectrometry 306 (2011) 37–43

Contents lists available at ScienceDirect

International Journal of Mass Spectrometry

journal homepage: www.elsevier.com/locate/ijms

Demonstration of on-line desalination for LC–MS using phosphate adsorption onto TiO_2-coated magnetic microparticles within a microchannel

Yoshitake Akiyama[a,*], Yutaka Takahashi[a,1], Issei Akutagawa[b], Akira Ono[b], Keisuke Morishima[c], Kazuhiro Chiba[b]

[a] Advanced Technology Division, JEOL Ltd., 3-1-2 Musashino, Akishima, Tokyo 196-8558, Japan
[b] Laboratory of Bio-organic Chemistry, Tokyo University of Agriculture and Technology, 3-5-8 Saiwai-cho, Fuchu, Tokyo 183-8509, Japan
[c] Department of Mechanical Systems Engineering, Tokyo University of Agriculture and Technology, 2-24-26, Naka-cho, Konganei, Tokyo 184-8588, Japan

ARTICLE INFO

Article history:
Received 25 September 2010
Received in revised form 6 June 2011
Accepted 7 June 2011
Available online 12 June 2011

Keywords:
Desalination
Phosphate buffer
TiO_2-coated magnetic microparticle
Microchannel

ABSTRACT

Phosphate buffer used commonly in liquid chromatography (LC) separation is not appropriate for mass spectrometry (MS) with an electrospray ionization source because nonvolatile salts in the buffer prevent sample molecules from being ionized. We have newly developed a desalination interface device (DID) for LC–MS using the specific adsorption of phosphate onto TiO_2-coated magnetic microparticles (TCMMPs). The TCMMPs which adsorb phosphate onto their own surface are collected by magnetic force in the microchannel of the DID and removed. The DID successfully collected almost all TCMMPs and the remaining phosphate rate was 15.1%. The signal-to-noise (S/N) ratio in the extracted ion chromatogram of reserpine obtained by LC-DID–MS was increased 5.3-fold compared to the one obtained by LC–MS. Our results indicate that the DID should be a powerful tool allowing phosphate buffer use in an on-line LC–MS system.

1. Introduction

Liquid chromatography coupled with mass spectrometry (LC–MS) is one of the most powerful analytical tools available today and it is applied in various fields, such as organic synthesis, drug development, food inspection, and biomolecular analysis [1]. LC–MS equipped with an electrospray ionization (ESI) source is most commonly used because ESI leads to less fragmentation than other ionization techniques and has broad utility. Phosphate buffer is commonly used in LC separation due to its wide-range buffering capacity and low UV absorption. Unfortunately, nonvolatile buffers such as phosphate buffer are inappropriate for ESI, since the MS signal slowly disappears due to accumulation of solid salts in the entrance cone of the MS though spectra are obtained initially. The phosphate not only precipitates and deposits around the orifice of the MS but also prevents the sample from being ionized when sample solution is evaporated in the ESI source [2–4]. Therefore, the sample has to be separated under volatile mobile phase, such as ammonium acetate or the nonvolatile salt has to be removed from the sample solution after separation.

However, the mobile phase often cannot be changed. For instance, when an unidentified peak in the ultra violet absorption spectrum is found after LC separation with the phosphate buffer, the fraction of the peak will often be analyzed by MS to obtain more information about the peak such as molecular weight and chemical structure. However, the phosphate salt included in the fraction has to be removed before analysis by MS. If the mobile phase in LC is changed to a volatile mobile phase, it will be difficult to find the same unidentified peak as the one obtained under the phosphate buffer condition because the elution position may be changed [5]. Therefore, it is desirable to develop an on-line device to remove nonvolatile salt between the LC and MS systems.

There have been numerous studies to remove nonvolatile salts from sample solutions, in which various methods were employed such as size exclusion chromatography (SEC) [6–8], reversed-phase liquid chromatography (RP-LC) [9,10], two-dimensional liquid chromatography (2D-LC) [11,12], C18-loaded pipette tips or a nanospray [13], liquid–liquid extraction using laminar flow in a microchannel [14], and dialysis [15,16]. Some of them were designed for on-line desalting of minute amounts of protein samples [8,13], which is incompatible with continuous running at a high flow rate around 200 μL/min needed for LC–MS. Wilson and Konermann [17] reported on-line rapid desalination for a protein solution based on liquid–liquid extraction using a microchannel laminar flow, by which nonvolatile salt was removed at a rate of around 90%. This strategy is also inapplicable for low molecular-weight compounds such as pharmaceuticals.

* Corresponding author. Current address: Department of Mechanical Systems Engineering, Tokyo University of Agriculture and Technology, 2-24-26, Naka-cho, Konganei, Tokyo 184-8588, Japan.
E-mail address: aki520227@gmail.com (Y. Akiyama).
[1] Current address: MS-Solutions Co. Ltd., 3-10-90 Fujimi-cho, Higashimurayama, Tokyo 189-0024, Japan.

1387-3806/$ – see front matter © 2011 Elsevier B.V. All rights reserved.
doi:10.1016/j.ijms.2011.06.005

Phosphate ions are known to be adsorbed strongly onto most metal oxides including TiO_2 [18]. Recently, this affinity has been used to collect phosphopeptide from crude extraction of biological samples and to enrich it [19,20]. In particular, TiO_2-coating magnetic (Fe_3O_4/TiO_2 core/shell) microparticles (TCMMPs) have been employed to collect and enrich phosphopeptide, because the TCMMPs conjugated to the phosphopeptide molecules can be collected readily from the sample solutions in a microtube or microwell by employing a magnetic field [21,22]. On the other hand, for continuous flow within a microchannel, magnetic micro and nano particle separations have also been achieved by application of a magnetic field [23,24].

Here we propose to employ TCMMPs in continuous flow within a microchannel as a desalination interface device (DID) so as to remove phosphate salt from sample solution after LC and before MS using an ESI source. In this study, we designed a microfluidic device equipped with magnets and confirmed its performance by measuring particle concentration and phosphate adsorption rate. We used reserpine as a sample and compared the analytical results by LC–MS with the DID and without it.

2. Methods

2.1. Experimental setup

The DID configuration is shown in Fig. 1a. The dynamic mixer (dead volume: 15 μL) was equipped with a heater and was connected to the microfluidic device by a polyetheretherketone (PEEK) tube (diameter: 0.25 mm). The microfluidic device consisted of top and bottom aluminum plates with a semicircular channel (diameter: 0.5 mm) and oblique access holes (diameter: 0.5 mm). A polytetrafluoroethylene (PTFE) sheet which had a mechanically produced penetrated straight groove of 0.5 mm width and 30 mm length (Fig. 1b) was sandwiched between the top and bottom aluminum plates. The surfaces of the aluminum plates were coated with PTFE. A Y-shaped microchannel was formed by the sandwich of the middle PTFE sheet with the two aluminum plates. The upper outlet of the microchannel was connected to the MS by another PEEK tube (diameter: 0.13 mm) and the lower outlet was the waste drain. One or three neodymium magnets (diameter: 14 mm; height: 10 mm) were set under the Y-junction. A bolt-clamped langevin type transducer (BLT) (Izumi Giken, Japan) was attached to the top plate of the microfluidic device.

The desalination mechanism of the DID was as follows. First, sample flowing from the LC was mixed with an ethanol dispersion of TCMMPs in the dynamic mixer. Then, the mixture was introduced into the microfluidic device which had a Y-shaped microchannel with two outlets. While the sample mixture was in the dynamic mixer and the microchannel, the phosphate salt in it was adsorbed onto the surface of the TCMMPs. At the Y-junction, the TCMMPs were collected on the lower side of the channel by the magnetic force of the neodymium magnets and sample solution without TCMMPs flowed along the upper side. To prevent the main part of the microchannel from being blocked by aggregates of TCMMPs, the microfluidic device was vibrated at 28 kHz by the BLT. The BLT was driven by a sine wave of 28 kHz and 300 V (peak-to-peak) which was obtained by amplifying signals generated by a function generator (Hewlett Packard, USA). A piezoelectric driver M-2682 (MESS-TEK, Japan) was used to amplify the signals and drive the BLT.

2.2. Preparation of TCMMPs

TCMMPs were prepared by a coprecipitation method [25,26]. First, 264.65 g of $FeSO_4{\cdot}7H_2O$ and 7.48 g of $FeCl_3{\cdot}6H_2O$ were dissolved in 200 mL of deionized water. Then, 23 mL of 28% ammonium water were added with stirring and magnetite (Fe_3O_4) particles were obtained. The particles were readily isolated using a magnet and then were washed repeatedly with ethanol (3 times) and distilled water (3 times) to remove any unreacted impurities. Next, the particles were coated with TiO_2 as follows [27]. The particles were redispersed in 250 mL of ethanol by sonication. A mixture of 30 mL of 33.3% (w/w) $Ti(OEt)_4$ solution in ethanol and 3 mL of water was added, and the particle dispersion liquid was stirred for 30 min. The particle dispersion was concentrated once and taken to dryness using an evaporator to strengthen the cross-linking of TiO_2 onto the surfaces of the particles. After TiO_2 coating, the particles were again washed repeatedly with ethanol (3 times) and distilled water (3 times). Finally, after filtration through a nylon mesh (pore size: 40 μm), the filtrate was dried overnight using an evaporator to yield TCMMP powder. The TCMMP powder was dispersed at the concentration of 3.0 wt% in ethanol by sonication for less than 1 min and used as a dispersion. The particle size distribution was measured by dynamic light scattering with a MicroTrac MT3000 (Nikkiso, Japan).

2.3. Measurement of particle concentration

The particle concentration was determined by measuring turbidity of sample solutions that included dispersed TCMMPs. The turbidities of known concentrations of particle suspensions between 0.0005 and 0.01 wt% were measured at 650 nm with a spectrophotometer V-660 UV/VIS (JASCO, Japan). By plotting the absorbance, the following equation was obtained: $Abs = 65.8 \times c$ ($r^2 = 0.9994$), where c and Abs correspond to particle concentration (wt%) and absorbance at 650 nm, respectively. Water and 3 wt% TCMMP dispersion were introduced into the DID at the same rate of 200 μL/min. Solutions flowing from the upper outlet to the MS was collected for 3 min. Their particle concentrations were calculated using the calibration curve. Based on the results, the remaining particle rate flowing from the upper outlet was determined by dividing the amount of the TCMMP from the upper outlet by the total amount of the TCMMP.

2.4. Measurement of phosphate concentration

In flowing adsorption experiments, 5 mM phosphate solution and 3% (w/w) TCMMP dispersion were introduced into the DID at the same rate of 200 μL/min and solution flowing from the upper outlet to the MS was collected for 1 min. In experiments on batch adsorption, 5 mM phosphate solution and 3% (w/w) TCMMP dispersion were mixed in equal amounts, and shaken for 2 min. After shaking, the TCMMPs were attracted to the bottom by a magnet and the supernatant was collected.

The molybdenum blue method [28] was used to determine phosphate concentration. The method is described briefly as follows. Potassium antimony tartrate solution was prepared by dissolving 1.551 g $K(SbO)C_4H_4O_6{\cdot}3H_2O$ in water and diluting to 500 mL. Ammonium molybdate solution was prepared by dissolving 20 g $(NH_4)_6Mo_7O_{24}{\cdot}4H_2O$ in water and diluting to 500 mL. The reaction mixture was prepared by mixing 50 mL of 2.5 M sulfuric acid solution, 5 mL of the potassium antimony tartrate solution, 15 mL of the ammonium molybdate solution, and 30 mL of 0.1 M ascorbic acid solution. One hundred microliter of the reaction mixture and 500 μL of sample solution were mixed. Absorbance at 880 nm was measured with the spectrophotometer 10 min after mixing. Phosphate concentration was calculated based on a calibration curve, which was drawn using standard phosphate solution for each experiment. Phosphate remaining rate was obtained by dividing the remaining amount by the total amount.

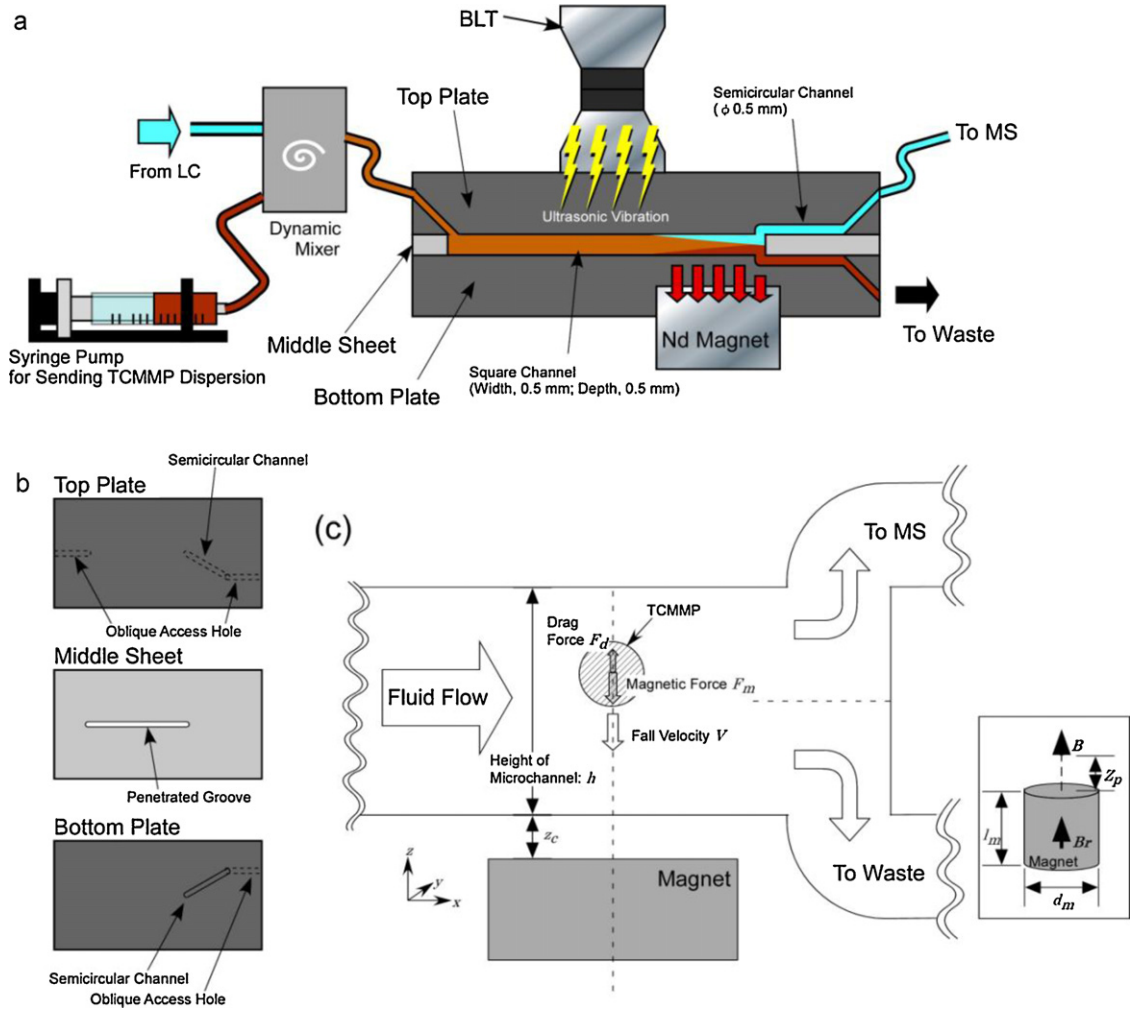

Fig. 1. Schematic diagram of the DID. The DID consists of a dynamic mixer, a microfluidic device (cross-sectional view), one or three neodymium magnets, and a bolt-clamped langevin type transducer (BLT). (b) Top views of top and bottom aluminum plates and middle PTFE sheet. (c) Cross-sectional scheme for theoretical model to estimate fall time of TCMMPs. The inset indicates the parameters of a neodymium magnet.

2.5. On-line MS analysis

The DID was connected between the LC and MS systems, and a sample was analyzed using phosphate buffer. The DID was connected to the MS by a polyetheretherketone (PEEK) tube (diameter: 0.13 mm). Another PEEK tube (diameter: 0.25 mm) was connected to the lower outlet (waste drain). The flow between the drain channel and the channel to the MS was equalized by adjusting the length of the PEEK tube for the waste drain. MS analysis was done with a JMS-T100LP (JEOL, Japan) consisting of a time of flight mass spectrometer equipped with an ESI source and an Agilent 1200 liquid chromatograph (Agilent Technologies, USA). Eluent A consisted of aqueous 2.5 mM phosphoric acid and 2.5 mM sodium dihydrogen phosphate, whereas eluent B was acetonitrile–water (80:20) containing 2.5 mM phosphoric acid and 2.5 mM sodium dihydrogen phosphate. Separation was done at the mobile phase flow rate of 200 μL/min using a Mightysil RP-18 column (Kanto Kagaku, Japan). The column was equilibrated with mixed eluent containing 98% eluent A and 2% eluent B. A sample was injected, and a linear gradient to 100% eluent B in 5 min was applied. Mass spectra were obtained with the ESI positive mode. Data acquisition and data analysis were performed using Masscenter software (JEOL, Tokyo, Japan). An extracted ion chromatogram obtained from 0.5 to 1 min was used as noise to calculate a signal-to-noise (S/N) ratio.

Next, the influence of only TCMMPs misled into the MS system was evaluated. The TCMMP solutions were prepared by suspending TCMMPs into ethanol at 0.05 or 0.10 wt%. Ten microliter of reserpine (100 ppb) solutions were injected into the LC–MS under the same conditions as above except for the mobile phase. In these experiments, 0.1% formic acid was used instead of phosphate buffer. Before injecting into the MS, TCMMP solution at the flow rate of 50 μL/min was mixed using a T-junction. As a result, the mixed solutions included TCMMPs at 0, 0.01, or 0.02 wt% for MS analysis.

3. Theory

Magnetic particles are attracted toward the bottom of the microchannel by magnetic force while they are flowing in the microchannnel. According to the simulation results we obtained using Ansys CFD software (Ansys Inc., USA), there was no eddy around the Y-junction and the fluid was divided into two pseudo-channels by the center plane (Fig. 2). Therefore, the TCMMPs below the center plane of the microchannel at the Y-junction will drain to the lower outlet as waste. Namely, all the TCMMPs having the fall time shorter than the time needed to pass through the area over the magnets will be collected into the drain, and some of the other

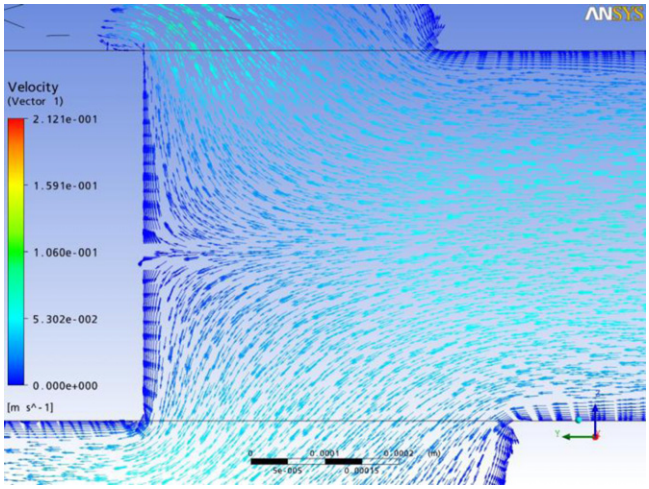

Fig. 2. Fluid simulation results on the vertical plane around the Y-shaped junction of the DID. The simulation was done for the viscosity of an ethanol–water solution (1:1 by volume) under a laminar flow condition. The vertical plane extends perpendicular to the centerline of the microchannel. Directions and colors of the arrows show direction and velocity of the fluid. The fluid was sent from right to left. It was confirmed that the fluid over the center plane flowed into the channel to the MS and the fluid below the center plane flowed into the waste drain.

TCMMPs with longer fall times will not be collected, but will flow into the outlet leading to the MS.

Fall time of TCMMPs from the top to the middle of the channel was estimated in a simplified model (Fig. 1c). Buoyant force was negligible compared with the magnetic force. Fluid flows in x and y directions and ascending flow caused by the falling TCMMPs were ignored to simplify the model. Magnetic flux density B above a cylindrical magnet is shown as a function of distance Z from the surface of the magnet in Fig. 1c inset and given by the following equation [29].

$$B = B_r \left(\frac{Z_p + l_m}{\sqrt{4(Z_p + l_m)^2 + d_m^2}} - \frac{Z_p}{\sqrt{4Z_p^2 + d_m^2}} \right) \quad (1)$$

According to Eq. (1), the magnetic flux density at a distance 2.25 mm from the surface of the magnet is 0.34 T, and the magnetization of TCMMPs will be saturated. Therefore, the magnetic force F_m acting on a TCMMP is proportional to the gradient of the magnetic flux density B when the magnetization of the TCMMPs reaches saturation M_{sat} and it is given by [30]

$$F_m = V(M_{sat} \cdot \nabla B) \quad (2)$$

Table 1
Minimum diameters of TCMMP collected completely by DID under each set of conditions.

Number of magnets	3	3	1	1
Height of microchannel (mm)	0.5	1.0	0.5	1.0
Minimum diameter (μm)	0.74	0.75	0.79	0.81

where V is the volume of a TCMMP. The volume V can be substituted by $\pi d_p^3/6$, where d_p is the diameter of a TCMMP. The drag force can be calculated with Stokes Law and the magnetic particle is accelerated in a very short time to its maximum velocity. Therefore, v can be expressed as

$$v = \frac{d_p^2}{18\eta}(M_{sat} \cdot \nabla B) \quad (3)$$

where η corresponds to dynamic viscosity of the fluid. If we consider that the TCMMPs fall just along the central axis of the magnet and we neglect the force in the x and y directions, fall time from the top to the center of the microchannel T is obtained by integration of $1/v_z$ from the top to the center of the microchannel

$$T = \int_{z_b+h/2}^{z_b+h} \frac{1}{v_z} dz$$

where z and h correspond to the distance from the surface of the magnet of the bottom of the microchannel and the height of the microchannel, respectively.

The relationship between d_p and T was calculated by Maxima, a computer algebra system [31], for each case of h = 0.5 and 1 mm when Br of the neodymium magnet, M_{sat} of TCMMPs, width of the microchannel w, and the distance from the surface of the magnet to the bottom of the microchannel z were set to 1.2 T, 4.8×10^5 A/m [32], 0.5 mm, and 1.25 mm, respectively. Assuming that the velocity profile was flat, for a 400 μL/min flow rate, we obtained transportation times to pass through the area over the magnet (12 mm) of 0.45 and 0.9 s, respectively, when h = 0.5 and 1 mm.

4. Results and discussion

4.1. Particle collection capacity of DID

Particle size is one of the most important factors on which the attracting force applied by a magnet depends. The particle size distribution is shown in Fig. 3. The relationship between the particle size and fall time under each set of conditions was obtained by a theoretical estimation (Fig. 4). The smallest collectable particle sizes (as minimum diameter) are summarized in Table 1. According

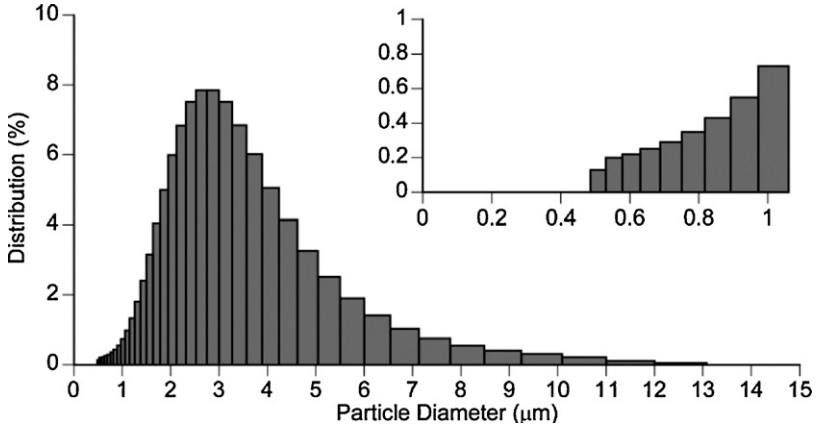

Fig. 3. Distribution of TCMMPs synthesized in this study. The inset is an enlarged graph around the smallest particles. TCMMPs particle were distributed over a wide range of diameters from 0.53 to 13.08 μm.

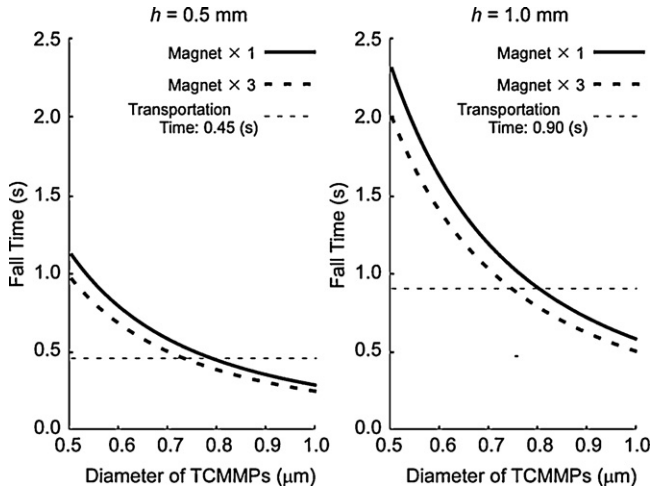

Fig. 4. Estimated fall time as a function of diameter of TCMMPs. The left and right graphs show data for two heights of the microchannel $h = 0.5$ and 1.0 mm, respectively.

to these results, the particle remaining rate would be approximately less than 1% in all cases. The height of the microchannel had little effect on the collectable particle size. Though the magnetic flux density in the microchannel increased when the height of the microchannel was lowered, the effect almost disappeared by decreasing the transportation time of the TCMMPs over the magnet. Since adding more magnets affected only the magnetic flux density in the microchannel, the smallest collectable size was only lowered from 0.79 to 0.74 μm when the height was 0.5 mm. The difference in the smallest collectable particle sizes under these conditions was hardly affected and was less than 0.5% according to the particle distribution in Fig. 3.

Transparent perfluoroalkoxyalkane (PFA) tubes (inner diameter: 0.5 mm) were connected to the upper and lower outlets of the microfluidic device and flowing fluid in each PFA tube was observed with a stereomicroscope (MZ16F, Leica, Germany). We confirmed that almost all TCMMPs were collected into the lower outlet (waste drain) under all conditions. The experimental results of the particle remaining concentration of the DID for each set of conditions are shown in Fig. 5. The TCMMPs could be collected very efficiently and the remaining particle rate was 1.23% when three

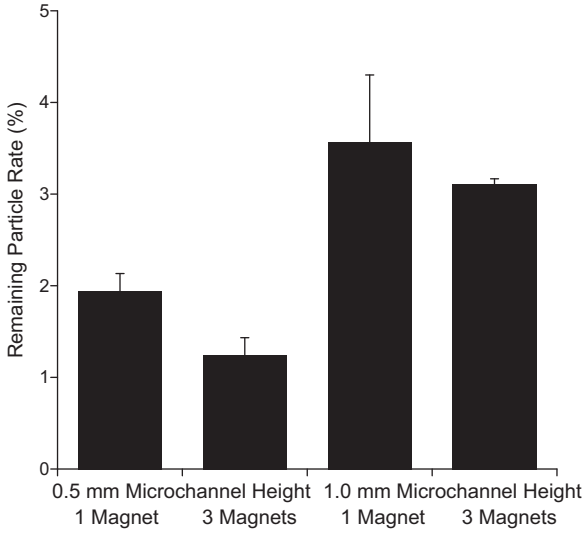

Fig. 5. Experimental results of particle remaining rate for each set of conditions. The remaining concentrations were less than 4% ($n = 6$, error bar: SD).

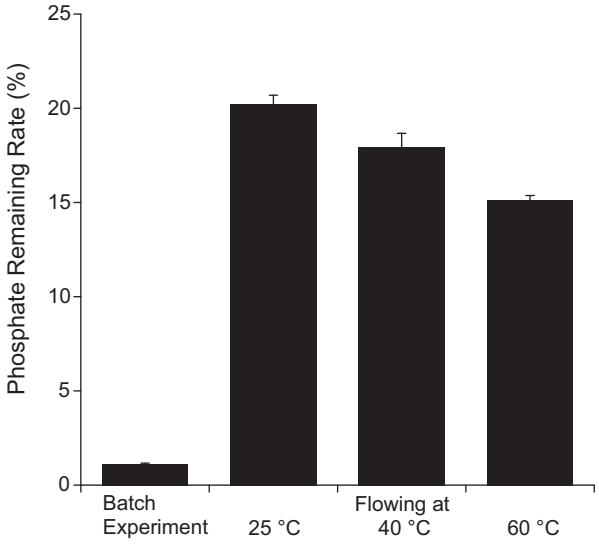

Fig. 6. Phosphate remaining rates measured by the molybdenum blue method. Though phosphate was almost adsorbed completely in the batch experiments, phosphate adsorption rates in the flowing experiments were more than 15% ($n = 3$, error bar: SD).

magnets were used and the height of the microchannel was 0.5 mm. We applied these conditions in experiments hereafter. The particle remaining rates for three magnets were lower than those for one magnet regardless of the height of the microchannel. However, unlike the theoretical estimation, the height of the microchannel influenced the remaining rates more than the number of magnets. These results should be due to partial blocking of the microchannel by aggregated particles attracted by the magnetic force though the surface of the microchannel was coated with PTFE and the DID was vibrated ultrasonically. The linear flow velocity is inversely proportional to the height of the microchannel. The higher the microchannel is, the more easily the particles adhere to the bottom of the microchannel. In fact, we often found a sludge of particles on the groove in the PTFE sheet when disassembling the DID after experiments. In all cases, the experimental particle remaining rate was less than the theoretical one. The results should be not only due to the sludge of particles mentioned above, but also due to upward flow generated by falling particles. Since the downward flow is generated by viscosity when many particles fall, upward flow must exist elsewhere. When a particle has a long falling distance, it may be easily caught in the upward flow.

4.2. Phosphate adsorption capacity of DID

The experimental results of phosphate adsorption rates are shown in Fig. 6. In the batch adsorption experiments at room temperature, almost all phosphate was adsorbed onto the TCMMPs and the phosphate remaining rate was 1.1%. In the flowing experiment at 25 °C, the remaining rate was 20.2%. In order to improve the rate, the dynamic mixer was heated to 60 °C. As a result, the remaining rate was increased to 15.1%, which was almost the same as the result by liquid–liquid extraction using a microchannel laminar flow of 10% [17]. The dynamic mixer was not heated above 60 °C because the boiling point of ethanol aqueous solution is around 80 °C [33]. The result for the flowing experiment at 60 °C was still 14% lower than the batch experiment results; the adsorption time was estimated as 3.7 s by dividing the dead volume of the DID (24.6 μL) by the flow rate (400 μL/min), and this time was much shorter than that of the batch experiments. The adsorption rate could be raised by increasing the adsorption time and improving

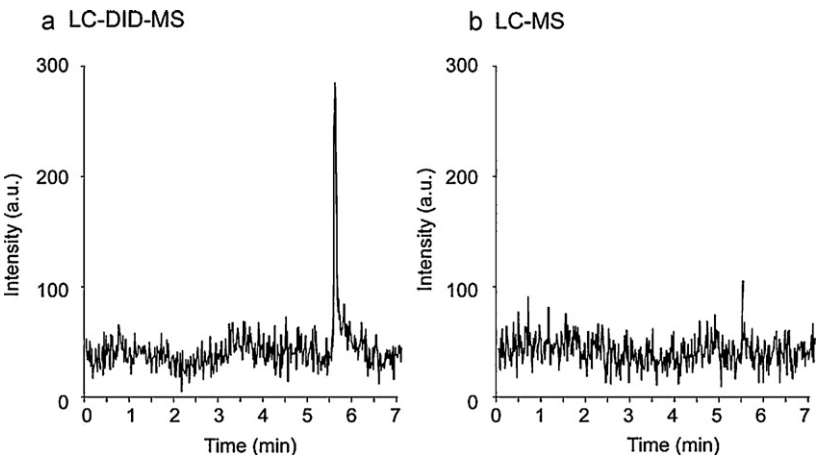

Fig. 7. Extracted ion chromatograms of reserpine by (a) LC-DID–MS and (b) LC–MS. The respective S/N ratios were 22.9 and 4.3 and the peak widths were 0.20 min and 0.05 min.

the dynamic mixer. In the following on-line analysis by LC-DID–MS, the dynamic mixer was heated to 60 °C.

4.3. On-line analysis by LC-DID–MS

To inspect the capability of the DID, 10 μL of reserpine solution (1 ppm) was injected into the LC-DID–MS and the LC–MS. No peak for reserpine was distinguished in the total ion chromatograph by either LC-DID–MS or LC–MS owing to the large background noise. The reserpine peak was detected in both extracted ion chromatograms obtained by LC-DID–MS and LC–MS (Fig. 7). In particular, the phosphate suppressed the peak intensity strongly (Fig. 7b). Although the results in the previous sections showed the DID could not collect all the TCMMPs and could not adsorb phosphate completely, the S/N ratio with DID was increased 5.3 times over that without the DID. The peak intensity with DID must be decreased by not only remaining phosphate but also remaining TCMMPs. The influence of only TCMMPs misled into the MS system was evaluated by interfusing TCMMPs artificially into the sample solution between the LC and MS systems. The peak intensity of the extracted ion chromatogram decreased as the particle concentration was increased (Fig. 8a). Calculation of the peak area showed a linear relationship between the particle concentration and peak area (Fig. 8b). By assuming linearity, the peak area would be 590 when TCMMPs were misled into the MS system at 0.037 wt% (remaining particle rate: 1.23%). Therefore, the peak area by LC-DID–MS increased by about 5-fold if the TCMMPs were removed completely.

On the other hand, the peak tail by LC-DID–MS was 4 times longer than that by LC–MS. The peak tailing should be caused by the dynamic mixer because it was hardly observed when only the DID was connected between the LC and MS systems. Additionally, nonspecific adsorption onto TiO_2 and sample loss when collecting TCMMPs should be considered. By quantitative analysis using MS, we confirmed that reserpine was adsorbed partly onto TiO_2 nonspecifically and the adsorption rate depended on the samples (manuscript in preparation). In particular, attention should be paid to this nonspecific adsorption when a sample with phosphate or carboxyl group is analyzed [18]. More detailed work is necessary to resolve the peak tailing and the nonspecific adsorption. Additionally, the current DID has to drain half of the sample to collect a sufficient amount of TCMMPs. This issue can be resolved by collecting TCMMPs under two-phase flow; for instance, by dispersing TCMMPs into a hydrophobic solvent such as cyclohexane. TCMMPs will go into the hydrophilic phase and adsorb phosphate when the TCMMP dispersion and aqueous sample solution are mixed since the surfaces of the TCMMPs are hydrophilic. Next, a two-phase flow is formed by introducing the TCMMP dispersion and the aqueous sample solution into the DID. Finally, the TCMMPs are collected in the hydrophobic phase by the magnetic force. In this way, the sample aqueous solution which does not include TCMMPs and phosphate will flow into the MS.

The sample mixture can be separated by LC using formic acid instead of phosphate buffer and the S/N ratio in the MS will increase significantly, however, formic acid may change the order of the elution. When there are unidentified peaks in the ultraviolet absorption spectrum obtained after the LC, the DID will give LC users a chance to analyze these peaks by MS. These results indicate that this technique to remove phosphate from buffer continuously has enough potential to apply it for LC–MS and the DID will enable LC–MS users to utilize phosphate buffer solutions on-line.

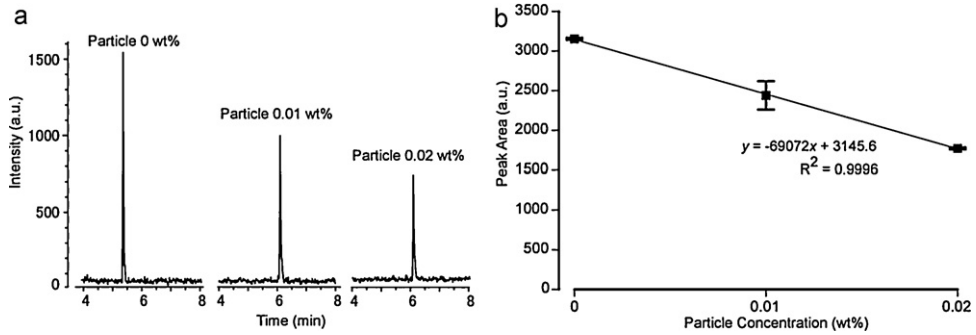

Fig. 8. Influence of misled TCMMPs into the MS system. (a) Extracted ion chromatograms of reserpine when the TCMMPs interfused at the final concentrations of 0, 0.01, and 0.02 wt%. (b) Peak areas of extracted ion chromatograms of reserpine in (a) ($n = 3$, error bar: SD).

5. Conclusions

In this study, we designed and fabricated the DID for LC–MS based on a theoretical simulation. The remaining particle and phosphate rates that the DID achieved under the optimized conditions were 0.037% and 15.1%, respectively. According to the analysis results by MS, the DID improved S/N ratios in extracted ion chromatograms. For reserpine, the S/N ratio in the extracted ion chromatogram increased 5.3-fold using the DID. These results indicate that the DID should be a powerful tool to allow phosphate buffer to be used in LC–MS. Next, we need to mitigate peak tailing and deal with the issues of nonspecific adsorption of a sample onto TCMMPs, undesired flow of TCMMPs into the MS system, and unadsorbed phosphate flowing into the MS system.

Acknowledgements

This work was financially supported by the NEDO Foundation (Grant for Practical Application of University R&D Results under the Matching Fund Method).

References

[1] J.H. Gross, Mass Spectrometry: A Textbook, Springer, Berlin, 2004.
[2] T.L. Constantopoulos, G.S. Jackson, C.G. Enke, Effects of salt concentration on analyte response using electrospray ionization mass spectrometry, J. Am. Soc. Mass Spectrom. 10 (1999) 625–634.
[3] C. Hao, R.E. March, T.R. Croley, J.C. Smith, S.P. Rafferty, Electrospray ionization tandem mass spectrometric study of salt cluster ions. Part 1 – investigations of alkali metal chloride and sodium salt cluster ions, J. Mass Spectrom. 36 (2001) 79–96.
[4] S. Zhou, M. Hamburger, Formation of sodium cluster ions in electrospray mass spectrometry, Rapid Commun. Mass Spectrom. 10 (1996) 797–800.
[5] W.J. Long, J.W. Henderson Jr., Separation of Salicylic Acid Impurities with Different Acid Mobile-Phase Modfiers, Agilent Publication 5989-7731EN, Agilent, Wilmington, DE, 2009, http://www.chem.agilent.com/Library/applications/5989-7731EN.pdf.
[6] M.L. Shen, L.M. Benson, K.L. Johnson, J.J. Lipsky, S. Naylor, Effect of enzyme inhibitors on protein quaternary structure determined by on-line size exclusion chromatography–microelectrospray ionization mass spectrometry, J. Am. Soc. Mass Spectrom. 12 (2001) 97–104.
[7] J. Cavanagh, R. Thompson, B.G. Bobay, L.M. Benson, S. Naylor, Stoichiometries of protein–protein/DNA binding and conformational changes for the transition-state regulator AbrB measured by pseudo cell-size exclusion chromatography–mass spectrometry, Biochemistry 41 (2002) 7859–7865.
[8] J. Cavanagh, L.M. Benson, R. Thompson, S. Naylor, In-line desalting mass spectrometry for the study of noncovalent biological complexes, Anal. Chem. 75 (2003) 3281–3286.
[9] W.M. Niessen, State-of-the-art in liquid chromatography–mass spectrometry, J. Chromatogr. A 856 (1999) 179–197.
[10] J. Abian, A.J. Oosterkamp, E. Gelpi, Comparison of conventional, narrow-bore and capillary liquid chromatography/mass spectrometry for electrospray ionization mass spectrometry: practical considerations, J. Mass Spectrom. 34 (1999) 244–254.
[11] Y. Oda, N. Mano, N. Asakawa, Quantitation of platelet-activating factor in biological samples using liquid chromatography/mass spectrometry with column-switching technique, Anal. Biochem. 231 (1995) 141–150.
[12] R.N. Rao, R.M. Vali, D.D. Shinde, On-line 2D-LC–ESI/MS/MS determination of rifaximin in rat serum, Biomed. Chromatogr. 23 (2009) 1145–1150.
[13] N. Lion, J. Gellon, H. Jensen, H.H. Girault, On-chip protein sample desalting and preparation for direct coupling with electrospray ionization mass spectrometry, J. Chromatogr. A 1003 (2003) 11–19.
[14] Y. Takahashi, R. Sakai, K. Sakamoto, Y. Yoshida, M. Kitaoka, T. Kitamori, On-line high-throughput ESIMS detection of a reaction product using synthesis and extraction microchips, J. Mass Spectrom. Soc. Jpn. 54 (2006) 19–24.
[15] N.C. van de Merbel, Membrane-based sample preparation coupled on-line to chromatography or electrophoresis, J. Chromatogr. A 856 (1999) 55–82.
[16] F. Xiang, Y. Lin, J. Wen, D.W. Matson, R.D. Smith, An integrated microfabricated device for dual microdialysis and on-line ESI-ion trap mass spectrometry for analysis of complex biological samples, Anal. Chem. 71 (1999) 1485–1490.
[17] D.J. Wilson, L. Konermann, Ultrarapid desalting of protein solutions for electrospray mass spectrometry in a microchannel laminar flow device, Anal. Chem. 77 (2005) 6887–6894.
[18] P.A. Connor, A.J. McQuillan, Phosphate adsorption onto TiO_2 from aqueous solutions: an in situ internal reflection infrared spectroscopic study, Langmuir 15 (1999) 2916–2921.
[19] G.T. Cantin, T.R. Shock, S.K. Park, H.D. Madhani, J.R. Yates, Optimizing TiO_2-based phosphopeptide enrichment for automated multidimensional liquid chromatography coupled to tandem mass spectrometry, Anal. Chem. 79 (2007) 4666–4673.
[20] T.E. Thingholm, T.J.D. Jorgensen, O.N. Jensen, M.R. Larsen, Highly selective enrichment of phosphorylated peptides using titanium dioxide, Nat. Protoc. 1 (2006) 1929–1935.
[21] C. Chen, Y. Chen, Fe_3O_4/TiO_2 core/shell nanoparticles as affinity probes for the analysis of phosphopeptides using TiO_2 surface-assisted laser desorption/ionization mass spectrometry, Anal. Chem. 77 (2005) 5912–5919.
[22] Y. Li, X. Xu, D. Qi, C. Deng, P. Yang, X. Zhang, Novel $Fe_3O_4@TiO_2$ core–shell microspheres for selective enrichment of phosphopeptides in phosphoproteome analysis, J. Proteome Res. 7 (2008) 2526–2538.
[23] M. Kersaudy-Kerhoas, R. Dhariwal, M. Desmulliez, Recent advances in microparticle continuous separation, IET Nanobiotechnol. 2 (2008) 1–13.
[24] I. Hsing, Y. Xu, W. Zhao, Micro- and nano-magnetic particles for applications in biosensing, Electroanalysis 19 (2007) 755–768.
[25] Y. Sun, X. Ding, Z. Zheng, X. Cheng, X. Hu, Y. Peng, Magnetic separation of polymer hybrid iron oxide nanoparticles triggered by temperature, Chem. Commun. 26 (2006) 2765–2767.
[26] M. Iijima, Y. Mikami, T. Yoshioka, S. Kim, H. Kamiya, K. Chiba, Rapid magnetic catch-and-release purification by hydrophobic interactions, Langmuir 25 (2009) 11043–11047.
[27] M. Holgado, A. Cintas, M. Ibisate, C.J. Serna, C. López, F. Meseguer, Three-dimensional arrays formed by monodisperse TiO_2 coated on silica spheres, J. Colloid Interface Sci. 229 (2000) 6–11.
[28] M. Radojević, V.N. Bashkin, Practical Environmental Analysis, Royal Society of Chemistry, Cambridge, UK, 1999.
[29] G.P. Hatch, R.E. Stelter, Magnetic design considerations for devices and particles used for biological high-gradient magnetic separation (HGMS) systems, J. Magn. Magn. Mater. 225 (2001) 262–276.
[30] R. Derks, A. Dietzel, R. Wimberger-Friedl, M. Prins, Magnetic bead manipulation in a sub-microliter fluid volume applicable for biosensing, Microfluid. Nanofluid. 3 (2007) 141–149.
[31] The Maxima computer Algebra System. http://maxima.sourceforge.net/.
[32] L. Ramajo, A. Cristóbal, P. Botta, J. Porto López, M. Reboredo, M. Castro, Dielectric and magnetic response of Fe_3O_4/epoxy composites, Compos. Appl. Sci. Manuf. 40 (2009) 388–393.
[33] R.C. Weast, Handbook of Chemistry and Physics, 44th ed., Chemical Rubber Co., Cleveland, OH, 1962.